nature communications

Article

https://doi.org/10.1038/s41467-024-53961-4

Distributed direct air capture of carbon dioxide by synergistic water harvesting

Received: 21 July 2024

Accepted: 29 October 2024

Published online: 11 November 2024

Check for updates

Yongqiang Wang[1,2], Longbing Qu[1], Hui Ding[2] ✉, Paul Webley[3] ✉ & Gang Kevin Li[1] ✉

Adsorption-based direct air capture (DAC) of carbon dioxide, using chemisorbents like solid amines, has been widely recognized as a sustainable measure to contain atmospheric CO_2 concentrations. However, the productivity and economic viability of DAC have been compromised by the high energy consumption for regenerating the adsorbents. Here, we show that by synergistically harvesting water and carbon dioxide from the atmosphere, we can regenerate the unit using in situ vapor purge at low energy and capital cost. The desorption of CO_2 is substantially enhanced in the presence of concentrated water vapors at around 100 °C, concurrently producing 97.7% purity CO_2 and fresh water without the use of vacuum pumps and steam boilers. Moreover, we demonstrate that the DAC prototype can also be powered by sunlight, which recovers 98% of the adsorbed CO_2, with 20% less energy demand, enabling sustainable carbon capture from air in a real distributed manner.

To achieve the climate goal of limiting global warming to below 1.5 °C, relying solely on traditional carbon capture technology to reduce emissions and mitigate the rate of CO_2 concentration increase may prove insufficient[1–4]. The urgent need to reverse the rising trend of CO_2 concentrations has created a strong demand for large-scale implementation of negative emissions technologies[5–7]. Direct air capture of CO_2 from the atmosphere has gained significant attention for achieving negative emissions[8–10]. DAC is advantageous for its potential to operate anywhere on earth, allowing for distributed carbon capture and CO_2 production. When combined with naturally distributed energy sources like solar and wind, DAC can sustainably provide the essential chemical feedstocks required for green fuel production.

Among the various DAC technologies, the adsorption-desorption process using solid adsorbents is particularly promising due to its relatively low regeneration temperature[11–13]. The selection of adsorbents and processes for DAC is constrained by the moisture and low concentration of CO_2 in the air (around 400 ppm)[11]. For physisorbents like 13X zeolite, the air needs to be dried in advance to avoid the competitive adsorption of atmospheric water and CO_2[14]. The application of physisorbents is constrained in cold conditions to reduce the energy consumption required for water removal[15,16]. Therefore, chemisorbents, particularly solid amine sorbents with large heat of adsorption (60–100 kJ mol^{-1}) and high CO_2 selectivity, are commonly employed in DAC due to the promoted CO_2 adsorption under humid conditions[17,18]. However, regenerating chemisorbents is energy-intensive due to the strong affinity of amine groups with CO_2. Considering the required scale of DAC deployment, the development of a regeneration technology with enhanced efficiency and reduced carbon footprint is essential for ensuring the sustainability of direct air capture[17,19,20].

Typically, the regeneration of chemisorbents in DAC requires elevating the temperature to above 100 °C using a heater, and reducing the partial pressure of CO_2 using a vacuum pump, both serving as the driving force for adsorbent regeneration[21,22]. To address this, temperature vacuum swing adsorption (TVSA) processes are commonly used to achieve CO_2 capture from air[6,17,23,24]. Nevertheless, the typical desorption pressure range of 5 to 30 kPa in the TVSA process can only release 30–50% of the adsorbed CO_2, resulting in low carbon dioxide productivity and hence a high capital cost[22,25,26]. To promote

[1]Department of Chemical Engineering, The University of Melbourne, Parkville, VIC, Australia. [2]School of Environmental Science and Engineering, Tianjin University, Tianjin, China. [3]Department of Chemical and Biological Engineering, Monash University, Clayton, VIC, Australia. ✉e-mail: dinghui@tju.edu.cn; paul.webley@monash.edu; li.g@unimelb.edu.au

CO_2 desorption and improve the working capacity, several strategies have been employed, including raising the desorption temperature, reducing the desorption pressure, and/or implementing steam stripping[26,27]. However, these approaches result in elevated energy consumption as well as increased operating and capital costs, such as the expenses associated with the vacuum pump. In particular, enhancing regeneration through high-temperature steam stripping requires a designated steam boiler that not only increases the capital cost of DAC but also limits the potential deployment of DAC under various scenarios due to constraints of fresh water supply.

The objective of this study is to develop an alternative method to desorb CO_2 in DAC, aiming to achieve a larger working capacity while minimizing energy consumption. In this work, we propose an in situ vapor promoted desorption (VPD) strategy to efficiently regenerate adsorbents and produce high purity CO_2 and fresh water from ambient air without requiring vacuum pumps or steam boilers. This approach substantially reduces CO_2 partial pressure during regeneration and recovers over 90% of the adsorbed CO_2 at 100 °C by in situ vapor purge using water harvested from the atmosphere. We demonstrate this in situ VPD process by constructing a solar-powered DAC prototype that uses sunlight as the sole energy source for adsorbent regeneration. This vapor promoted DAC process achieves much higher CO_2 working capacities in comparison with prevalent TVSA techniques, reducing energy consumption and realizing a low total cost of \$111–\$313 t^{-1}_{CO2}. In addition, the simultaneous production of water and carbon dioxide allows this DAC to be coupled with the CO_2 utilization processes, further improving the economic feasibility of direct air capture.

Results

Working principle of vapor promoted desorption

To evaluate the efficiency of a given desorption technology for DAC, we introduce a parameter termed Regeneration Efficiency (R), which quantifies the percentage of CO_2 that can be recovered from the adsorbents. R is defined by the equation:

$$R = \frac{W_c}{q_{ad}} \tag{1}$$

where W_c (mmol g^{-1}) is the CO_2 working capacity achieved using the given desorption technology, q_{ad} (mmol g^{-1}) represents CO_2 loadings on the adsorbent materials after adsorption. A higher regeneration efficiency enhances CO_2 productivity and reduces equipment volume, leading to decreased operating and capital costs for DAC. We evaluated the regeneration efficiency of the conventional TVSA process using CO_2 adsorption isotherm data (Supplementary Table 1) of a benchmark solid amine sorbent. As shown in Fig. 1a, the TVSA process requires elevated temperatures and reduced pressures for CO_2 desorption. Considering the thermal stability of the material and the desorption pressure achievable by regular vacuum pumps, reaching an R value > 0.6 is highly challenging.

To address the harsh conditions (Supplementary Fig. 1), we introduce in situ vapor promoted desorption to achieve efficient adsorbent regeneration with an R value exceeding 0.9. This VPD process promotes CO_2 adsorbent regeneration via in situ vapor purge using water harvested from the atmosphere. As shown in Fig. 1b,

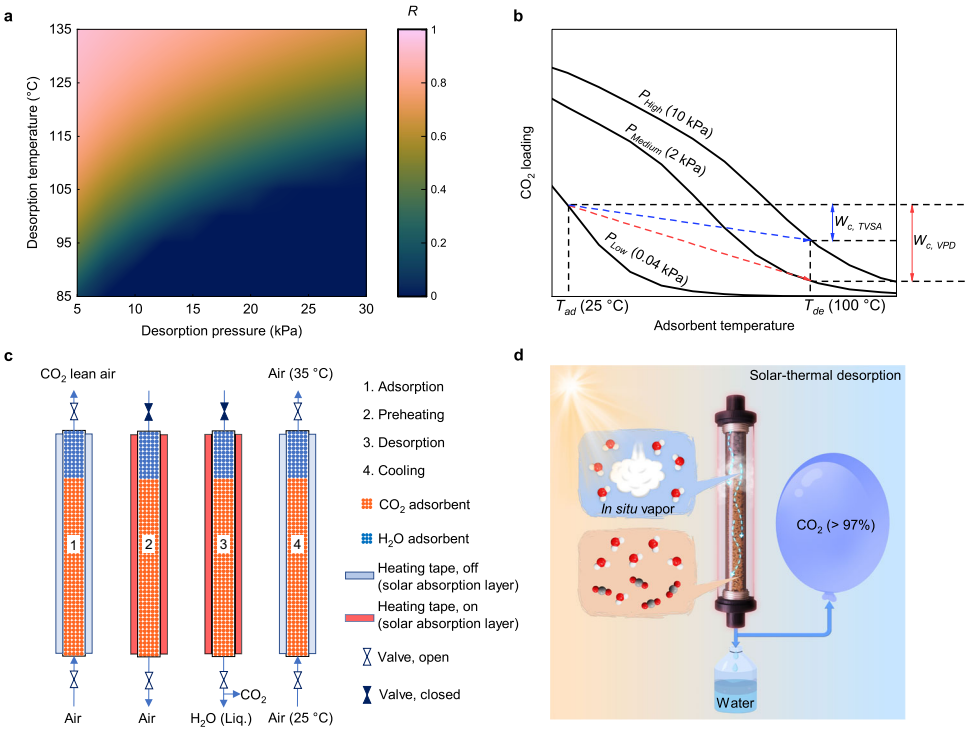

Fig. 1 | Working principle of vapor promoted desorption for DAC. a Calculated R values of conventional TVSA processes at various desorption temperatures and pressures, with fixed adsorption conditions of 25 °C and 400 ppm CO_2. **b** Working capacities of vapor promoted desorption ($W_{c,VPD}$) and TVSA ($W_{c,TVSA}$) processes calculated from the CO_2 adsorption isobar of a benchmark solid amine sorbent. P and T represent CO_2 partial pressure and desorption temperature, respectively. Assuming that adsorption is carried out at 25 °C with a CO_2 partial pressure of 0.04 kPa, while regeneration is conducted at 100 °C. Vapor promoted desorption, conducted without the use of vacuum conditions, results in a significant reduction in CO_2 partial pressure (around 2 kPa) due to the in situ purging effect of the generated water vapors. **c** Four-step DAC process including an adsorption step at ambient conditions, a preheating step for increasing temperatures, a desorption step for product collection, and a cooling step. **d** Schematic diagram of a solar-thermal desorption process based on in situ vapor purge. It is understood that the packing of the adsorbents in the column can be optimized for example into honeycomb structures to reduce the pressure drops; however, we emphasize the purpose of this study is to develop efficient regeneration methods and the configuration of adsorbents is not our focus. Source data are provided as a Source Data file.

https://doi.org/10.1038/s41467-024-53961-4

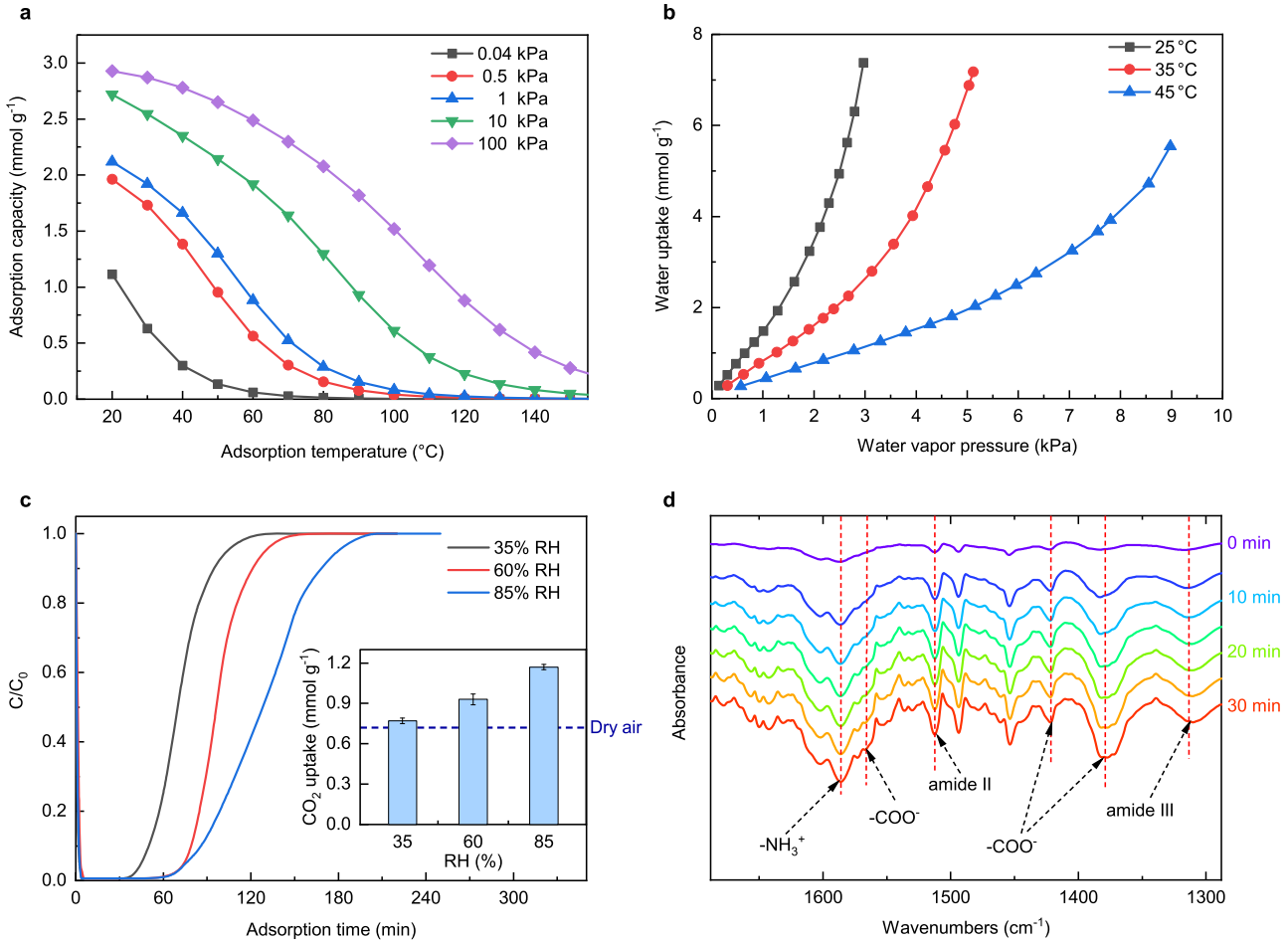

Fig. 2 | Adsorption properties of the primary amine-grafted resin. a CO_2 adsorption isobar of the amine-grafted resin. **b**, Water adsorption isotherm of the amine-grafted resin at 25 °C, 35 °C and 45 °C. **c** CO_2 breakthrough curves of the amine-grafted resin at 28 °C and 410 ppm, with a gas hourly space velocity (GHSV, based on the volume of resin) of 12000 h^{-1}. The inset shows atmospheric CO_2 adsorption capacities under dry and different humidity conditions. Error bars represent the standard deviation of at least three independent measurements. **d** In situ Fourier transform infrared spectroscopy (FTIR) spectra of the amine-grafted resin after 0, 5, 10, 15, 20, 25, and 30 min treatment in flowing N_2 atmosphere at 100 °C. The sample was pretreated with 25 °C and 30% RH air for 12 h. Source data are provided as a Source Data file.

compared with conventional TVSA with a desorption pressure of 10 kPa, our VPD process can significantly reduce CO_2 partial pressure by vapor purge, providing a tremendous driving force for CO_2 desorption, leading to an increased working capacity and regeneration efficiency.

The entire process is composed of four stages (Fig. 1c) namely, adsorption, preheating, desorption, and cooling. In the adsorption stage, two adsorbents sequentially packed in the column adsorb CO_2 and H_2O from the air. Subsequently, the temperature of the adsorbent bed is elevated through solar or electrical heating. The CO_2 and vapors with increased partial pressures displace air inside the column, thereby preventing oxidative degradation of the adsorbent at high temperatures. During the desorption stage, the increased vapor partial pressure reduces the carbon dioxide partial pressure and promotes the regeneration of solid amine sorbents. This desorption approach only requires thermal energy, which can be obtained from diverse sources like waste heat or sunlight, to raise the adsorbent temperatures and perform regeneration (Fig. 1d), eliminating the need for an external purge supply or vacuum pumps. The water in the product stream is easily condensed and separated, leaving high-purity CO_2. After collecting the products, fresh air is introduced to lower the adsorbent temperature and initiate the next adsorption cycle.

Adsorption properties

Type A silica gel and a primary amine-grafted resin were used as the water and CO_2 adsorbents for testing vapor promoted DAC, respectively. The resin exhibited an impressive CO_2 uptake capability of 1.11 mmol g^{-1} at 20 °C and 400 ppm (Fig. 2a and Supplementary Table 1). In Fig. 2b, the hydrophobic styrene-divinylbenzene structure of the resin resulted in limited water uptakes at low relative humidities (RH). By contrast, silica gel was able to adsorb more than 10 wt% water even under 30% RH conditions (Supplementary Fig. 2). The addition of silica gel could significantly increase the amount of co-adsorbed water, thus providing a solid foundation for vapor promoted desorption.

Moisture has been proven to significantly affect the CO_2 adsorption properties of solid amine sorbents[11,28]. The impact of moisture on CO_2 adsorption behaviors of the amine-grafted resin was studied by conducting breakthrough experiments at varying humidities (Supplementary Fig. 3). Compared with adsorption with dry air, the CO_2 uptakes at 35%, 60%, and 85% RH was observed to increase by 6.9%, 29.2%, and 62.5%, respectively (Fig. 2c and Supplementary Fig. 4). However, higher CO_2 uptakes and slower adsorption kinetics under high humidity conditions led to longer adsorption time for achieving adsorption equilibrium. The reduced adsorption rate at 85% RH might be attributed to mass transfer restrictions caused by the high water loadings.

https://doi.org/10.1038/s41467-024-53961-4

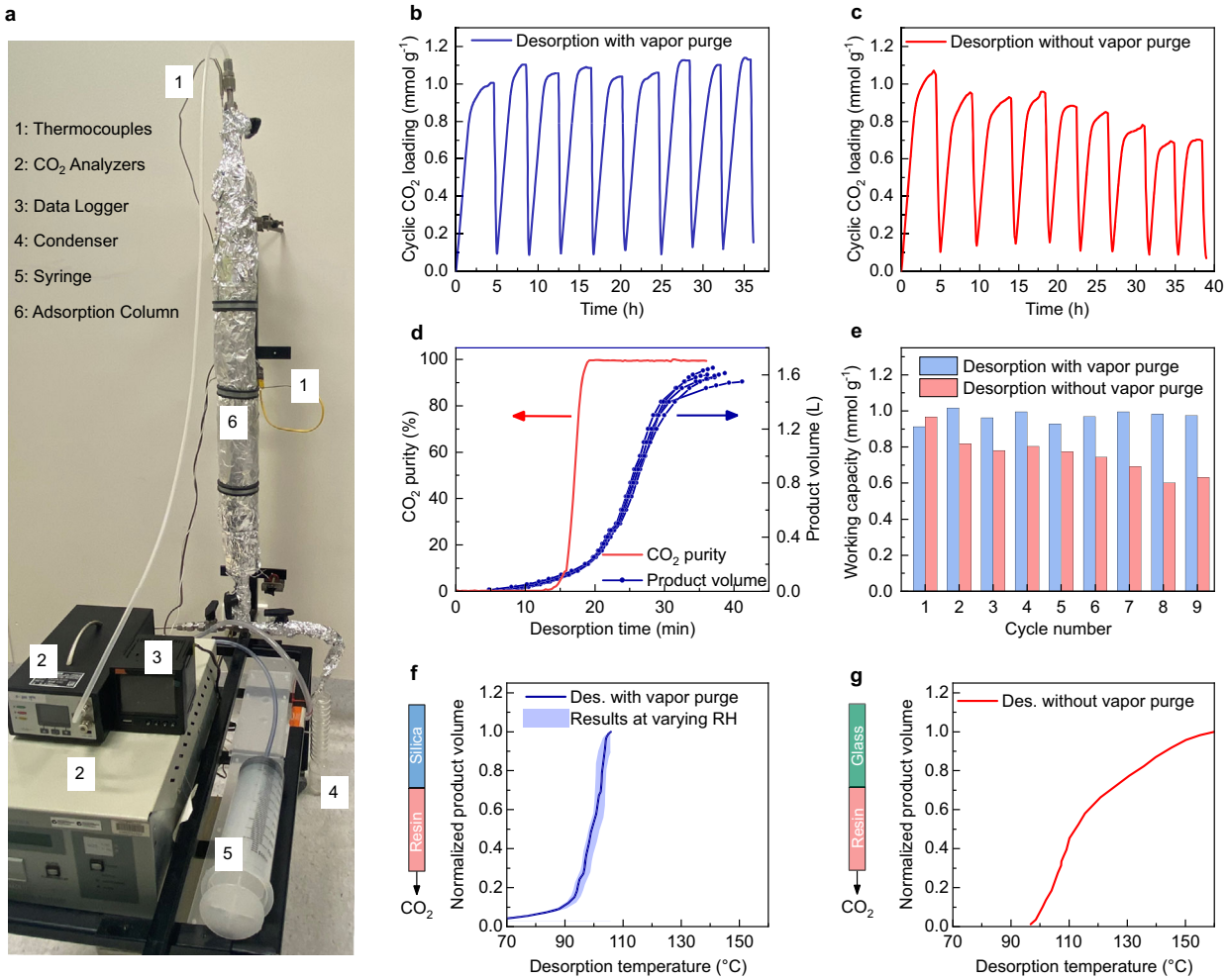

Fig. 3 | Performance of cyclic vapor promoted DAC in comparison to desorption without in situ vapor purge. a Experimental setup for vapor promoted DAC during the regeneration powered by electrical heating. Cyclic CO_2 loading profiles for desorption with (**b**) and without (**c**) in situ vapor purge during nine adsorption-desorption cycles. Adsorbents: 180 mL CO_2 capture resin and 180 mL silica gel. Fresh air at 27 °C with RH ranging from 35 to 60% was used as the feed stream with a GHSV of 10,000 h^{-1}. Desorption without in situ vapor purge was performed by replacing silica gel with glass beads. **d** Real-time CO_2 purity and product volumes of different cycles during VPD. **e** Cyclic working capacities calculated from the CO_2 loading profiles. **f** Normalized product volumes (ratios of collected product volume to final product volume) during desorption with in situ vapor purge under different desorption temperatures. The shaded areas illustrate the variations in results obtained under different relative humidities ranging from 35% to 60%. The solid line represents the experiment conducted under a relative humidity of 50%. **g** Normalized product volume during desorption without in situ vapor purge, when the adsorption was performed at 35% RH. Source data are provided as a Source Data file.

The mechanism of atmospheric CO_2 adsorption on the primary amine-grafted resin was investigated by recording the in situ FTIR spectra during N_2 purge (Fig. 2d). Before the analysis, the sample was pretreated with 25 °C and 30% RH air for 12 h, and carbamate species were found by FTIR spectra in Supplementary Fig. 5. Upon treating with 100 °C N_2 stream, the desorption of CO_2 was reflected in decreases of the absorptance at 1380, 1510 and 1584 cm^{-1}, corresponding to the symmetric stretching vibration of -COO^-, C-N stretching vibration (amide II) and antisymmetric deformation of NH_3^+ in ammonium carbamate structures, respectively[29–31]. The results suggested that the formation of ammonium carbamate was the dominant mechanism for atmospheric CO_2 adsorption at 30% RH using the primary amine-grafted resin.

Thermal stability can be a major concern for solid amine sorbents during regeneration[32]. Thermogravimetric analysis was conducted at different temperatures and atmospheres to assess the thermal stability of amines. The resin kept losing CO_2 sorption capacity after each desorption step at 110 °C in air, totaling more than 20% loss in 6 cycles (Supplementary Fig. 6). In contrast, at a desorption temperature of 70 °C, there wasn't any obvious loss of CO_2 sorption capacity, suggesting lower regeneration temperatures are critical to maintaining the performance of the resin for DAC. When pure CO_2 was used for the thermalgravimetric analysis instead of air, the resin kept stable at 120 °C after repeated cycles and degradation wasn't seen until the regeneration temperature reached 150 °C (Supplementary Fig. 7). From the in situ FTIR analysis in CO_2 atmosphere at 150 °C, we found that the deactivation was primarily caused by the formation of cyclic and open-chain ureas (Supplementary Fig. 8)[33].

Cyclic performance of in situ vapor promoted DAC

To study the cyclic stability and performance of solid amines under the condition of in situ vapor purge, silica gel was packed in the same column for adsorbing moisture from air and providing the in situ vapor, along with the CO_2 capture resin. The setup of the VPD process is shown in Fig. 3a and Supplementary Figs. 9, 10, where regeneration is achieved through electrical heating. At a feed gas hourly space velocity of 10,000 h^{-1}, each adsorption (~3 h) and desorption (~40 min) cycle can produce carbon dioxide at a productivity of 3.7–3.9 kg h^{-1} m^{-3}_{resin}

(Fig. 3b, c). The released CO_2 could reach a maximum purity of over 99% during VPD after 19 min preheating, as shown in Fig. 3d and Supplementary Movie 1. The collected products were further analyzed by gas chromatography, showing a CO_2 concentration of 97.7% and an O_2 concentration of 0.5%. The low concentrations of O_2 within the column could reduce the risk of amine oxidation during regeneration. Remarkably, our VPD process maintained a stable CO_2 working capacity of 0.9–1.0 mmol g^{-1} (Fig. 3e) over nine cycles, as nearly all the CO_2 products could be collected at temperatures below 105 °C (Fig. 3f). The high CO_2 productivity and working capacity achieved by in situ vapor purge can significantly reduce the capital cost associated with the expensive CO_2 adsorbents used in DAC.

By contrast, the DAC without using in situ vapor purge, lost 40% of its working capacity at cycle 8, starting from 0.97 mmol g^{-1} at cycle 1 (Fig. 3c and e). This low stability can be attributed to the significantly higher temperatures required, ranging from 130 to 150 °C, to achieve a similar product volume compared with VPD (Fig. 3g and Supplementary Fig. 11). These observations highlight the importance of in situ vapor purge in reducing the required regeneration temperatures for CO_2 desorption.

In the above setup using a resin volume fraction of 0.5, the amount of CO_2 desorbed was barely influenced by the feed air humidity, as shown in the shaded area of Fig. 3f. This suggests the amount of in situ vapor could be far more than sufficient for purge. To analyze the necessary amount of co-adsorbed water or silica gel for in situ vapor purge, VPD was investigated under various relative humidities (Fig. 4), and in the meantime, the resin volume fraction was increased to 0.8 (320 mL CO_2 capture resin and 80 mL silica gel). Figure 4a and Supplementary Fig. 12 demonstrated stable CO_2 working capacities ranging from 0.85 to 1.00 mmol g^{-1} which is similar to the CO_2 working capacity in our earlier tests using a resin volume fraction of 0.5 (Fig. 3b). At elevated temperatures, the desorbed water first served as the vapors with high partial pressures over 95 kPa for in situ purge of CO_2 within the column (Fig. 4b). Then the vapor was condensed in the subsequent air-cooled condenser as fresh liquid water verified by the ^{1}H NMR results (Fig. 4c and Supplementary Movie 1). This gas/liquid separation allowed for the recovery of high concentration CO_2 products ranging from 4.5 to 5.0 g per cycle. Meanwhile, water productivity ranged from 5.0 to 6.5 g per cycle depending on the atmospheric humidity (Fig. 4a). It should be noted that only a small fraction of water (~22%) was desorbed, involved as vapors for performing in situ purge, and collected as a liquid product (Fig. 4d). Whereas the increased vapor pressure could substantially reduce the CO_2 partial pressure, releasing over 90% of the adsorbed CO_2 at temperatures below 110 °C (Fig. 4b and Supplementary Fig. 12).

For this in situ vapor purge with a resin volume fraction of 0.8, the required desorption temperatures for achieving different R values were determined by the amount of adsorbed water as shown in Supplementary Fig. 13 and Supplementary Methods. By increasing the molar ratio of equilibrium loading of adsorbed water to CO_2 (n_{water}/n_{CO2}), the desorption temperature could be lowered due to the increased quality of vapors generated for in situ purge. Based on this correlation between n_{water}/n_{CO2} and desorption temperatures, the regeneration efficiency R of VPD was estimated at different resin volume fractions, atmospheric humidities, and desorption temperatures to provide guidance for the operation of vapor promoted DAC (Fig. 4e). By adjusting the volume fraction of adsorbents, VPD can be applied in various climate environments, from arid to humid areas. Even in areas with low humidities of around 20–25%, typical to average air humidity in deserts[34], our VPD can still achieve a regeneration efficiency of 0.9, as demonstrated in the shaded area of Fig. 4e. In a more humid environment, for example, 50% relative humidity air, desorption temperature as low as 104 °C is highly effective in generating abundant vapors for in situ purge, releasing over 90% of the adsorbed CO_2. Both of the above examples do not need vacuum pumps for the regeneration of CO_2 adsorbents. When evacuation is applied, the desorption temperature can be further reduced in our VPD process. As shown in Fig. 4f, by applying a moderate vacuum of 50 kPa, we only need a regeneration temperature of 87 °C to recover 90% of the CO_2 from the column; or recover 80% of the CO_2 at 80 °C.

In general, for a given air humidity, we can adjust the resin volume fraction and the desorption temperature to achieve a high CO_2 capture performance using our VPD process (Fig. 4e and Supplementary Fig. 13), while considering the specific environmental conditions, such as weather and the temperature of the heat source available, at the location where DAC is conducted.

Solar-powered VPD prototype for DAC

As only low-grade heat is required to drive the VPD process, in addition to electrical heating, we also built a solar-powered VPD prototype which converts solar energy to thermal energy with high efficiencies. As shown in Fig. 5a and Supplementary Fig. 14, the prototype consists of a horizontal adsorption column coated in black and double-glazed with a transparent vacuum isolation and a parabolic solar concentrator with an optical concentration ratio of 1.9 (Fig. 5b). The photothermal conversion efficiency of the prototype was calculated to be 63.1% by monitoring the temperature changes of the column under solar irradiation (Fig. 5c). Additionally, a correlation was established between the solar flux and heating power of the prototype. Under a typical solar flux of 500 W m^{-2}, the prototype with a projected area of the black coating being 0.05 m^2, is capable of generating thermal energy equivalent to 30 W of electrical heating (Fig. 5d). A concept of a solar-powered DAC farm is illustrated in Fig. 5e, featuring an array of solar heating columns designed for capturing atmospheric carbon dioxide and moisture, while producing high purity CO_2 and water upon solar heating. This demonstration's ability to operate in distributed scenarios using only air and sunlight as inputs not only makes the DAC process more sustainable but also enables its deployment in remote areas without the need for extensive infrastructure.

To demonstrate the CO_2 capture performance of this solar-powered DAC prototype, three VPD tests were conducted using varying volumes of adsorbents under different weather conditions (Fig. 6 and Supplementary Fig. 15). After adsorbing atmospheric CO_2 and water, the DAC prototype was directly exposed to sunlight for VPD, generating 2.89, 5.11, and 7.24 g CO_2 per cycle using 200, 320, and 420 mL resin, respectively. Under moderate solar intensities ranging from 500 to 700 W m^{-2}, nearly all the adsorbed CO_2 was released ($R > 0.97$) within 50 min (Fig. 6b and Supplementary Fig. 15), driven by in situ vapor purge which was powered by solar heating at around 110 °C.

In temperature swing adsorption processes, the cooling step usually takes the longest time. Shortening the cooling time is critical to improving the overall productivity of the CO_2 capture. In this study, we noticed that the temperature of the double-layered column using both silica gel and resin decreased two times faster than that without silica gel layer. As shown in Fig. 6c, the former decreased from 113 °C to 68 °C within 120 s, while the latter only dropped to 92 °C. Such enhanced cooling is caused by the evaporation of water in the double-layered column, where the partial pressure of water is significantly reduced by the incoming air. As the column is cooled down to ambient, the equilibrium shifts towards the next cycle of water adsorption.

High energy consumption is another concern that compromises the economic feasibility of DAC. The energy consumption of this solar-powered VPD was calculated based on the photothermal conversion efficiency and solar intensities (Supplementary Methods). Figure 6d demonstrated that vapor promoted DAC required only 10.4 MJ kg^{-1}_{CO2} of thermal energy converted from sunlight for adsorbent regeneration. The sensible heat and latent heat needed to conduct the vapor promoted desorption were further analyzed (Fig. 6e and Supplementary Table 2). We found that the sensible heat for increasing the resin

https://doi.org/10.1038/s41467-024-53961-4

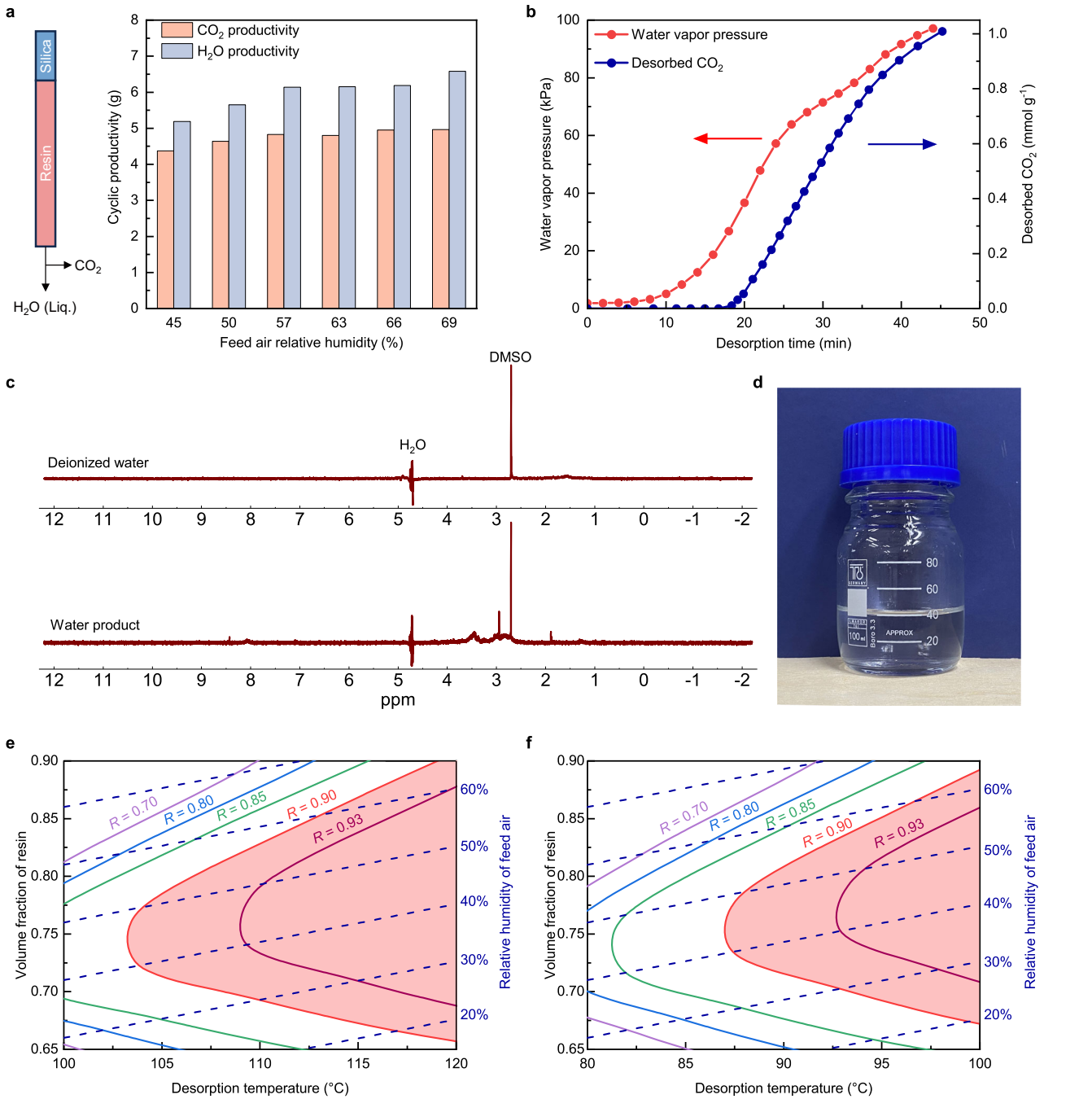

Fig. 4 | Cyclic CO_2 and water productivities, along with regeneration efficiency predictions for VPD. a Cyclic CO_2 and water productivities under different relative humidities. Adsorbents: 320 mL CO_2 capture resin and 80 mL silica gel. Fresh air at 27 °C with RH ranging from 45 % to 70 % was used as the feed stream with a GHSV of 5600 h^{-1}. **b** Amounts of desorbed CO_2 and partial pressures of water vapor inside the column during the regeneration stage. **c** ^{1}H NMR spectra for the high purity liquid water produced by our VPD process, in benchmark against deionized water. DMSO with 12 ppm concentration was employed as the reference. **d** Water products collected during vapor promoted desorption, with a pH range of 7–7.5. Predicting regeneration efficiency R of VPD under desorption pressures of 100 kPa (**e**) and 50 kPa (**f**), at given volume fraction of resin, desorption temperature, and relative humidity of feed air. Adsorption is assumed to be conducted at 28 °C and 410 ppm CO_2 under given humidity levels. The shaded red areas represent the recommended operating conditions for vapor promoted DAC with an R exceeding 0.9. Source data are provided as a Source Data file.

temperature and the latent heat for releasing the adsorbed water dominated the energy consumption and costs. This energy consumption would remain consistent regardless of the thermal energy sources applied, as they share the same mechanism for vapor promoted desorption. In comparison, the reported energy consumptions for TVSA and steam-assisted TVSA processes using the same resin as CO_2 adsorbent were in the range of 12–15 MJ kg^{-1}_{CO2}, including 0.5–1 MJ kg^{-1}_{CO2} of electrical energy for evacuation[17,26]. In comparison with other state-of-the-art regeneration processes like electrically driven temperature-swing desorption and pH-swing desorption[24,35], the VPD process also offers the advantages of zero electricity consumption and high product purity (Supplementary Table 3). This in situ vapor purge is better suited for direct air capture since it functions independently of external purge gas, steam, or water supplies.

https://doi.org/10.1038/s41467-024-53961-4

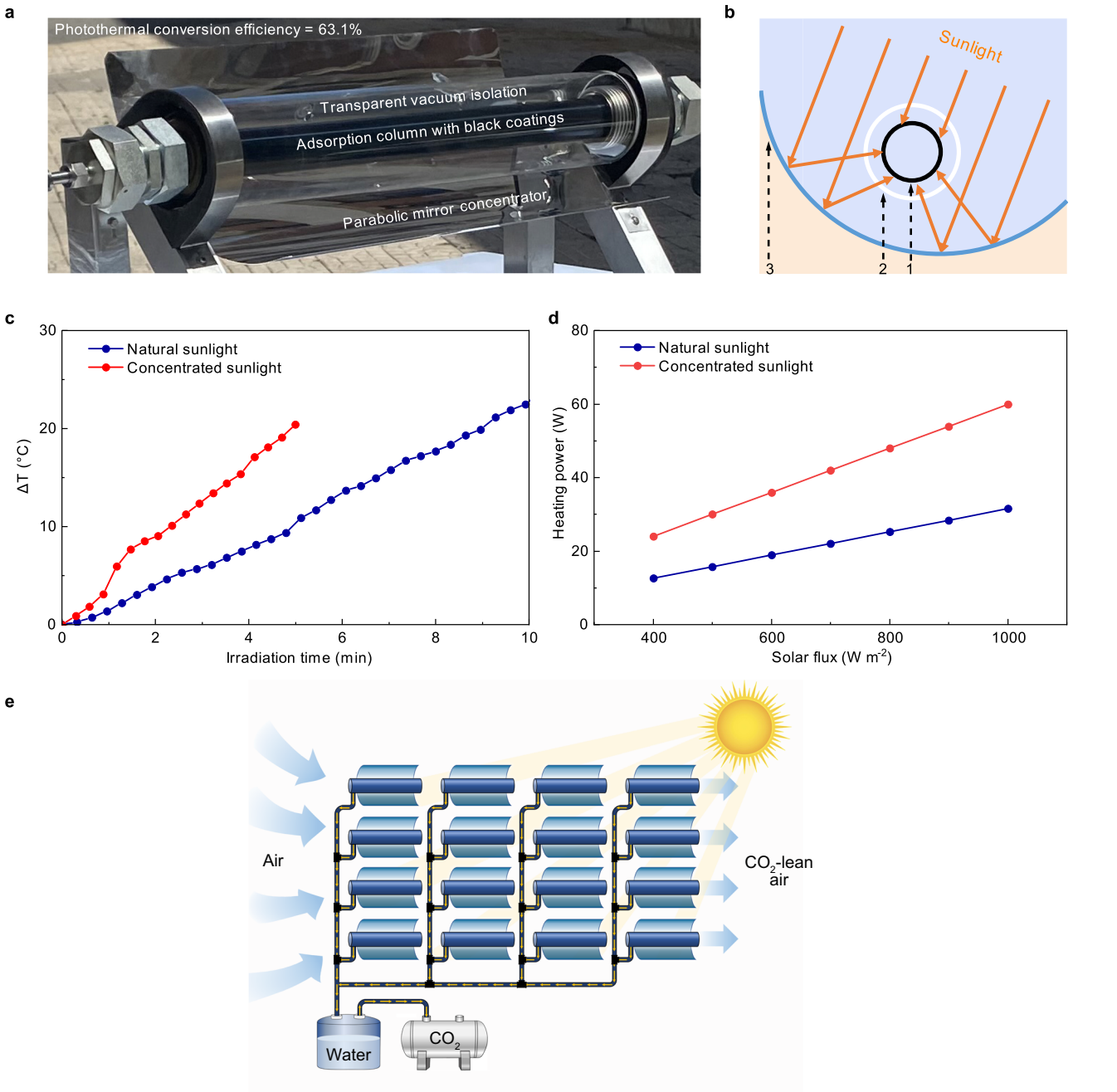

Fig. 5 | Solar heating performance of the photothermal DAC prototype. **a** Prototype of the photothermal DAC system including an adsorption column with black coatings for photothermal conversion, a transparent vacuum isolation for reducing heat loss, and a parabolic mirror concentrator. **b** Schematic diagram of the photothermal DAC prototype. 1. Adsorption column with black coatings; 2. Transparent vacuum isolation; 3. Parabolic mirror concentrator. **c** Temperature change profiles of the adsorption column under 600 W m^{-2} solar irradiation. The solid lines are guides to the eye. Concentrated sunlight was generated by the parabolic mirror concentrator. **d** Heating powers of the photothermal system under natural sunlight and concentrated sunlight. The solid lines are guides to the eye. **e** Conceptual illustration of solar-powered DAC farm capturing CO_2 and water from the natural wind flow. The adsorption and regeneration steps can be switched by rotating the solar concentrators to either shade or expose the columns to sunlight. Source data are provided as a Source Data file.

Furthermore, our vapor promoted DAC also eliminates the necessity for industrial steam boilers and vacuum pumps, leading to savings in both capital and operating costs.

The total cost of the vapor promoted DAC process, including capital expenditures (cost for air contactor and sorbents) and operational expenditures (energy costs)[17], is evaluated based on the cyclic results and energy consumption of VPD (Supplementary Methods and Supplementary Table 4). As shown in Supplementary Fig. 16, due to the high working capacity and CO_2 productivity realized by in situ vapor purge, the expense for the contactor generally remains below \$57 t^{-1}_{CO2} and accounts for less than 30% of the total cost. The stability of CO_2 adsorbents significantly influences the overall cost of DAC, especially when the lifetime is less than 5 years. Our VPD technique with stable cyclic performance may be a potential option to regenerate chemisorbents and avoid amine degradation, reducing the cost of replacing the expensive adsorbents used in DAC. An energy cost of \$29–\$144 t^{-1}_{CO2} is needed to supply the thermal energy required for vapor promoted desorption when the heat cost ranges from

https://doi.org/10.1038/s41467-024-53961-4

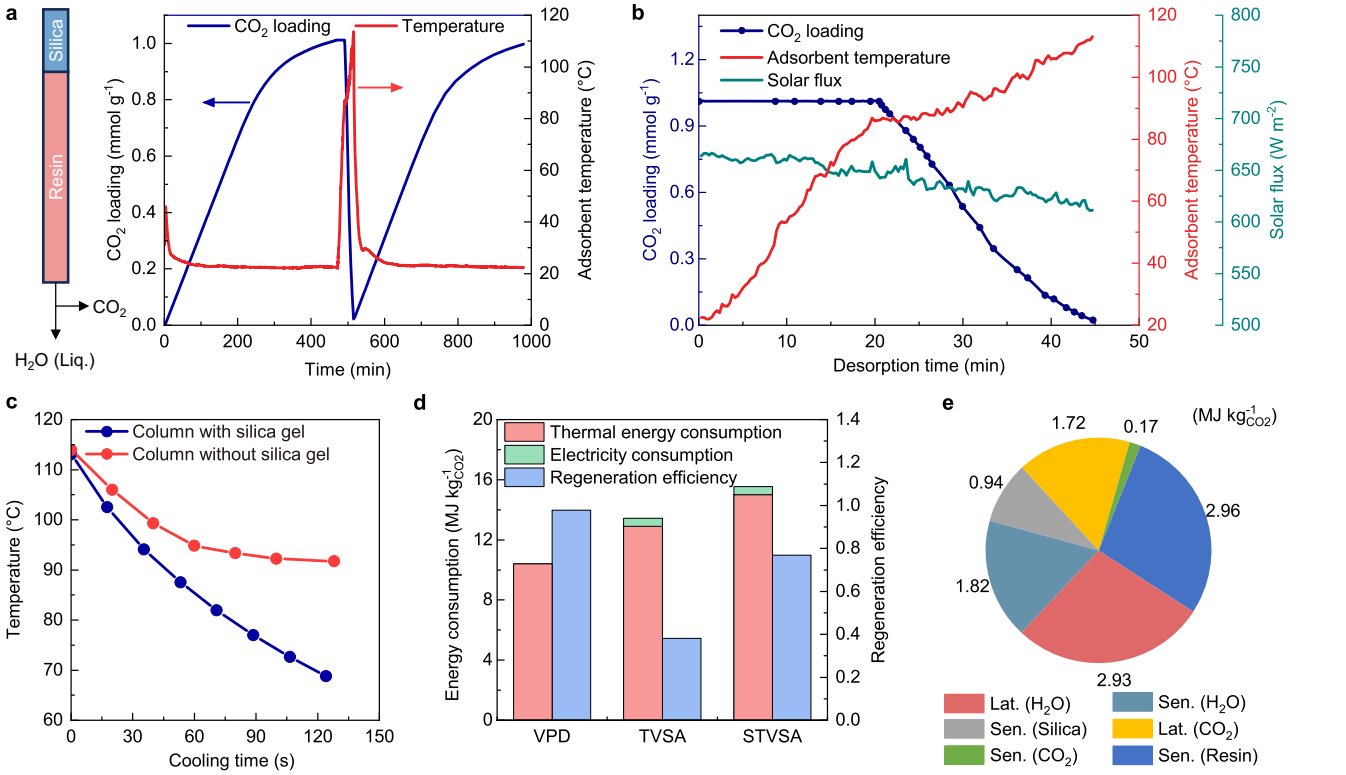

Fig. 6 | Performance of solar-powered VPD prototype for DAC. a CO_2 loading and adsorbent temperature profiles during the adsorption-desorption cycles. Solar-powered VPD with 320 mL amine-grafted resin and 80 mL silica gel, was tested at 56% RH and a GHSV of 3750 h^{-1} in Tianjin China (39°06'32.9"N 117°10'11.1"E) during May 2022. The performance of VPD under other weather conditions and adsorbent volume fractions can be found in Supplementary Fig. 15. **b** CO_2 loading, adsorbent temperature, and solar flux profiles during the solar-powered regeneration stage. **c** Temperature profiles of the resin in the columns with and without silica gel during the cooling process after solar-powered regeneration. The solid lines are guides to the eye. **d** Thermal energy consumption, electricity consumption, and regeneration efficiency *R* of VPD process, compared with reported TVSA and steam-assisted TVSA (STVSA) processes using the same CO_2 adsorbent (Ref. 26). **e** Breakdown of thermal energy consumption for adsorbent regeneration in the VPD process. Lat. represents the heat associated with the desorption of CO_2 and water. Sen. denotes the thermal energy needed to increase the temperature of sorbent materials and adsorbed molecules. Source data are provided as a Source Data file.

$0.01–$0.05 kWh^{-1}. Thus, the use of low-grade waste heat and renewable energy in DAC is beneficial for reducing energy costs and minimizing additional CO_2 emissions from the capture process. In summary, the vapor promoted DAC can be operated at a total cost of $111–$313 t^{-1}_{CO2}, depending on the contactor cost, heat cost, and sorbent lifetime (Supplementary Fig. 16). The overall cost could be further reduced by developing adsorbents with better CO_2 uptakes and stability, and operating in situ vapor purge at lower temperatures to decrease the sensible heat demand.

Discussion

In this study, we developed a vapor promoted DAC to achieve high CO_2 working capacity with a low energy penalty through in situ purge of vapor synergistically harvested from the air. The process used double-layered amine-grafted resin and silica gel for adsorbing atmospheric CO_2 and water, respectively. During regeneration, water vapors desorbed from silica gel significantly reduced CO_2 partial pressures, promoting the desorption of carbon dioxide. The stable CO_2 working capacity, maintained at approximately 1.0 mmol g^{-1} after nine cycles, was achieved by in situ vapor purge at moderate regeneration temperatures of around 105 °C. In our VPD process, the temperature required to achieve a regeneration efficiency *R* was found to be determined by the molar ratio of equilibrium loading of adsorbed water to CO_2 (n_{water}/n_{CO2}). This correlation was further used to predict the VPD performance under varying adsorbent volume fractions and feed air humidities. The vapor promoted DAC demonstrated operational flexibility across a broad range of atmospheric humidities in both arid and humid environments, effectively releasing over 90% of the adsorbed CO_2 from the chemisorbent at 103–120 °C. By applying a moderate vacuum of 50 kPa, the regeneration temperature can be efficiently reduced to about 85 °C. To minimize the carbon footprint associated with raising the adsorbent temperature and generating vapors, solar energy was used to power VPD with a photothermal conversion efficiency of 63.1%. Even under low solar intensities of 600 W m^{-2}, around 98% of the adsorbed CO_2 could be released within 50 minutes.

The energy consumption for VPD was calculated to be 10.3 MJ kg^{-1}_{CO2}, significantly lower than reported TVSA and steam-assisted TVSA processes using the same CO_2 adsorbent. More than half of the thermal energy was employed to increase the resin temperature and release the water adsorbed on silica gel. Compared with other electrically driven regeneration processes, the VPD provides a higher CO_2 product purity and only requires low-grade heat to perform the desorption. The overall cost of vapor promoted DAC ranges from $111 to $313 t^{-1}_{CO2} and is sensitive to sorbent lifetime and heat costs. More research should be conducted to further reduce the temperature required to generate in situ vapors and to develop stable amine structures resistant to thermal degradation. This work provides an alternative process for efficiently regenerating chemisorbents, concurrently achieving high CO_2 working capacity and low energy consumption, demonstrating the potential to reduce both operating and capital costs of DAC.

Methods

Materials

Lewatit VP OC 1065 (Lanxess) was used as the CO_2 adsorbent for direct air capture in this study. The material, which ranges in diameter from 0.3–1.2 mm, is a primary amine functionalized weakly basic anion exchange resin that has been identified as a promising adsorbent for DAC. To harvest atmospheric water and realize in situ vapor purge, we employed type A silica gel (Desicco) with a particle size of 3–5 mm as the water adsorbent. Prior to usage, the silica gel and resin were pretreated under vacuum at 110 °C and 80 °C, respectively.

Adsorption isotherms and characterizations

The CO_2 adsorption behavior of the amine-grafted resin is characterized using the following Dual-site Langmuir model[36], with the fitted parameters provided in Supplementary Table 1.

$$q_{CO_2} = \frac{q_1 K_1 P}{1 + K_1 P} + \frac{q_2 K_2 P}{1 + K_2 P} \tag{2}$$

$$K_1 = K_{0,1} \exp\left(\frac{-\Delta H_{ads,1}}{RT}\right) \tag{3}$$

$$K_2 = K_{0,2} \exp\left(\frac{-\Delta H_{ads,2}}{RT}\right) \tag{4}$$

The theoretical working capacity (W_c) of the amine-grafted resin is evaluated by the following equation,

$$W_c = q_{CO_2}\left(T_{ads}, P_{CO_2,ads}\right) - q_{CO_2}\left(T_{des}, P_{CO_2,des}\right) \tag{5}$$

$q_{CO_2}(T_{ads}, P_{CO_2,ads})$ and $q_{CO_2}(T_{des}, P_{CO_2,des})$ represent calculated CO_2 loadings under adsorption and desorption conditions based on the proposed isotherm model. P_{CO_2} and T are the CO_2 partial pressure and adsorbent temperature. For calculating the theoretical working capacity, T_{ads} and $P_{CO_2,ads}$ are fixed at 25 °C and 40 Pa, respectively.

The water adsorption isotherms of the amine-grafted resin and silica gel were measured at temperatures of 25, 40, and 55 °C with a Belsorp-MAX Analyzer. The samples were degassed for 12 h at 120 °C before measurement.

Fourier-transform infrared spectroscopy spectra were collected using a Nicolet iS50 FTIR Spectrometer. The thermal stability of the CO_2 capture resin was characterized using thermogravimetric analysis (TGA) with a Mettler Toledo TGA/DSC 1 under the designated atmosphere and conditions. In situ, FTIR was used to investigate the changes in surface species during the regeneration or deactivation of the amine-grafted resin with a Bruker Tensor 27 spectrometer. Before analysis, the sample was exposed to air at 25 °C and 30% RH overnight to adsorb CO_2 and H_2O. Then, the sample was treated with N_2 (99.99% purity) flow at 100 °C while spectra were recorded every 5 min. The CO_2-induced deactivation mechanism was investigated using in situ FTIR under a CO_2 (99.99% purity) atmosphere at 150 °C. The sample was treated with pure CO_2 at 80 °C for 3 h and at 150 °C for 15 min before analysis, with spectra collected every 60 min at 150 °C.

Breakthrough experiments

A stainless-steel tube of 8 cm in length and 1 cm in diameter was employed as the adsorption column to analyze the breakthrough curves for CO_2 adsorption (Supplementary Fig. 3). The adsorption temperature was controlled by a thermostat oven set to 28 °C. Compressed air with 410 ppm CO_2 was introduced to the adsorption column at a gas-hourly space velocity of 12,000 h^{-1}. A humidifier at 28 °C was used to control the relative humidity of the feed air. The outlet CO_2 concentrations were monitored by an infrared CO_2 sensor (Dynament, 0–1000 ppm), while two humidity sensors (Ningbo Keshun KS-SHT and Vaisala HMT338) continuously recorded the feed and outlet relative humidity. Breakthrough experiments were performed under different humidities to investigate the impact of varying humidities on CO_2 adsorption behavior.

Vapor promoted DAC

The schematic of the setup used for testing vapor promoted DAC is illustrated in Supplementary Fig. 10. Stainless steel columns, measuring 60 cm in length and 4 cm in diameter, were used as adsorption columns. Silica gel and CO_2 capture resin were packed sequentially within one adsorption column. Fresh air containing 410–450 ppm CO_2 first flowed over the resin, and subsequently over silica gel, for CO_2 and H_2O adsorption. GHSV was regulated by flow meters and ranged from 3000 to 10,000 h^{-1}. One of the air streams passed through a 27 °C humidifier to control the humidity of the feed gas. The outlet CO_2 concentrations were monitored by an infrared CO_2 sensor (Dynament, 0–1000 ppm), while the feed and outlet relative humidity were continuously recorded by two humidity sensors (Ningbo Keshun KS-SHT and Vaisala HMT338).

A thermal couple was placed at the center of the amine-grafted resin to monitor the temperature profile throughout the adsorption-desorption cycles. The CO_2 uptake ($q^{ads}_{CO_2}$, mmol g^{-1}) during the adsorption process was calculated based on the following equation[37],

$$q^{ads}_{CO_2} = \int_0^{t_{ads}} \frac{n_{air}\left(C_{CO_2,in} - C_{CO_2,out}\right)}{m} dt \tag{6}$$

where t_{ads} is the adsorption time, n_{air} is the flow rate of the inlet air, $C_{CO_2,in}$ is the atmospheric CO_2 concentration, $C_{CO_2,out}$ is the CO_2 concentration in the outlet gas and m is the mass of the amine-grafted resin. The water adsorption capacity is determined by the same calculation method.

Thermal energy, either supplied by electrical heating tapes or solar energy, was employed to regenerate the adsorbents and produce high purity CO_2 and water. The adsorption columns used for electrical and solar heating are illustrated in Supplementary Fig. 9. In this study, the electrical heating power applied was 90 W, while the solar flux typically ranged from 400 to 800 W m^{-2} for solar heating.

During the preheating and desorption steps, valve V1 was closed, and the double-layered column was directly connected to an air-cooled condenser for product collection (Supplementary Fig. 10). The preheating step, aimed at elevating the regeneration temperature to 90 °C, was initiated by either turning on the electrical heating or exposing the column to sunlight for solar heating. The solar flux was measured by a pyranometer (Renke, RS-RA). As the temperature of the adsorbent increased, the vapors in the product stream were collected as liquid water products by the air-cooled condenser, while the CO_2 product was collected using a syringe to record the product volume profile. The collected CO_2 product was then stored in gas sampling bags and analyzed using gas chromatography with a thermal conductivity detector. To monitor the real-time product purity, a CO_2 analyzer (Servomex 1440) was directly connected to the condenser and syringe. The volume profile of desorbed CO_2 can be expressed as,

$$V_{CO_2,t_{des}} = \int_0^{t_{des}} C_{CO_2,t} \frac{\partial V_{p,t}}{\partial t} dt \tag{7}$$

where $V_{CO_2,t_{des}}$ is the desorbed CO_2 volume at a certain desorption time (t_{des}), $V_{p,t}$ is the product volume at t, $C_{CO_2,t}$ is the real-time CO_2 purity of the product at t. Once the volume profile of desorbed CO_2 is obtained, the CO_2 loading of the amine-grafted resin during the desorption step can be determined.

The water product collected from the condenser was analyzed using ^{1}H NMR spectra (Varian VNMRS 600 MHz). To analyze the water vapor pressure inside the column during desorption, a humidity

sensor (Vaisala HMT338) was positioned within the column to monitor the humidity and temperature surrounding the amine-grafted resin. The water vapor pressure was calculated using the Antoine equation for vapor-pressure data[38]. After the desorption process, the adsorption column was purged with fresh air to rapidly decrease the adsorbent temperature and initiate the next adsorption cycle.

Reporting summary

Further information on research design is available in the Nature Portfolio Reporting Summary linked to this article.

Data availability

The data supporting the findings of this study are available within this paper and the Supplementary Information. Source data are provided with this paper.

References

1. Breyer, C., Fasihi, M., Bajamundi, C. & Creutzig, F. Direct air capture of CO_2: a key technology for ambitious climate change mitigation. *Joule* **3**, 2053–2057 (2019).
2. Tanzer, S. E. & Ramírez, A. When are negative emissions negative emissions? *Energ. Environ. Sci.* **12**, 1210–1218 (2019).
3. Rogelj, J. et al. Scenarios towards limiting global mean temperature increase below 1.5 °C. *Nat. Clim. Change* **8**, 325–332 (2018).
4. Vousdoukas, M. I. et al. Small island developing states under threat by rising seas even in a 1.5 °C warming world. *Nat. Sustain.* **6**, 1552–1564 (2023).
5. Erans, M. et al. Direct air capture: process technology, techno-economic and socio-political challenges. *Energ. Environ. Sci.* **15**, 1360–1405 (2022).
6. Deutz, S. & Bardow, A. Life-cycle assessment of an industrial direct air capture process based on temperature-vacuum swing adsorption. *Nat. Energy* **6**, 203–213 (2021).
7. van Vuuren, D. P., Hof, A. F., van Sluisveld, M. A. E. & Riahi, K. Open discussion of negative emissions is urgently needed. *Nat. Energy* **2**, 902–904 (2017).
8. Schäppi, R. et al. Drop-in fuels from sunlight and air. *Nature* **601**, 63–68 (2022).
9. Keith, D. W. Why capture CO_2 from the atmosphere? *Science* **325**, 1654–1655 (2009).
10. Brethomé, F. M., Williams, N. J., Seipp, C. A., Kidder, M. K. & Custelcean, R. Direct air capture of CO_2 via aqueous-phase absorption and crystalline-phase release using concentrated solar power. *Nat. Energy* **3**, 553–559 (2018).
11. Sanz-Pérez, E. S., Murdock, C. R., Didas, S. A. & Jones, C. W. Direct capture of CO_2 from ambient air. *Chem. Rev.* **116**, 11840–11876 (2016).
12. Goeppert, A., Czaun, M., Surya Prakash, G. K. & Olah, G. A. Air as the renewable carbon source of the future: an overview of CO_2 capture from the atmosphere. *Energ. Environ. Sci.* **5**, 7833–7853 (2012).
13. Zhu, X. et al. Recent advances in direct air capture by adsorption. *Chem. Soc. Rev.* **51**, 6574–6651 (2022).
14. Kumar, A. et al. Direct air capture of CO_2 by physisorbent materials. *Angew. Chem. Int. Ed.* **54**, 14372–14377 (2015).
15. Song, M. et al. Cold-temperature capture of carbon dioxide with water coproduction from air using commercial zeolites. *Ind. Eng. Chem. Res.* **61**, 13624–13634 (2022).
16. Fu, D. & Davis, M. E. Toward the feasible direct air capture of carbon dioxide with molecular sieves by water management. *Cell Rep. Phys. Sci.* **4**, 101389 (2023).
17. Sabatino, F. et al. A comparative energy and costs assessment and optimization for direct air capture technologies. *Joule* **5**, 2047–2076 (2021).
18. Alkhabbaz, M. A., Bollini, P., Foo, G. S., Sievers, C. & Jones, C. W. Important roles of enthalpic and entropic contributions to CO_2 capture from simulated flue gas and ambient air using mesoporous silica grafted amines. *J. Am. Chem. Soc.* **136**, 13170–13173 (2014).
19. Sutherland, B. R. Pricing CO_2 direct air capture. *Joule* **3**, 1571–1573 (2019).
20. Keith, D. W., Holmes, G., St. Angelo, D. & Heidel, K. A process for capturing CO_2 from the atmosphere. *Joule* **2**, 1573–1594 (2018).
21. Wijesiri, R. P., Knowles, G. P., Yeasmin, H., Hoadley, A. F. A. & Chaffee, A. L. Desorption process for capturing CO_2 from air with supported amine sorbent. *Ind. Eng. Chem. Res.* **58**, 15606–15618 (2019).
22. Elfving, J., Bajamundi, C., Kauppinen, J. & Sainio, T. Modelling of equilibrium working capacity of PSA, TSA and TVSA processes for CO_2 adsorption under direct air capture conditions. *J. CO2 Utilization* **22**, 270–277 (2017).
23. Wurzbacher, J. A., Gebald, C. & Steinfeld, A. Separation of CO_2 from air by temperature-vacuum swing adsorption using diamine-functionalized silica gel. *Energ. Environ. Sci.* **4**, 3584–3592 (2011).
24. Lee, W. H. et al. Sorbent-coated carbon fibers for direct air capture using electrically driven temperature swing adsorption. *Joule* **7**, 1241–1259 (2023).
25. Elfving, J. et al. Experimental comparison of regeneration methods for CO_2 concentration from air using amine-based adsorbent. *Chem. Eng. J.* **404**, 126337 (2021).
26. Bos, M. J., Pietersen, S. & Brilman, D. W. F. Production of high purity CO_2 from air using solid amine sorbents. *Chem. Eng. Sci.: X* **2**, 100020 (2019).
27. Stampi-Bombelli, V., van der Spek, M. & Mazzotti, M. Analysis of direct capture of CO_2 from ambient air via steam-assisted temperature-vacuum swing adsorption. *Adsorption* **26**, 1183–1197 (2020).
28. Young, J., García-Díez, E., Garcia, S. & van der Spek, M. The impact of binary water-CO_2 isotherm models on the optimal performance of sorbent-based direct air capture processes. *Energ. Environ. Sci.* **14**, 5377–5394 (2021).
29. Afonso, R., Sardo, M., Mafra, L. & Gomes, J. R. B. Unravelling the structure of chemisorbed CO_2 species in mesoporous aminosilicas: a critical survey. *Environ. Sci. Technol.* **53**, 2758–2767 (2019).
30. Bacsik, Z. et al. Mechanisms and kinetics for sorption of CO_2 on bicontinuous mesoporous silica modified with n-propylamine. *Langmuir* **27**, 11118–11128 (2011).
31. Danon, A., Stair, P. C. & Weitz, E. FTIR study of CO_2 adsorption on amine-grafted SBA-15: Elucidation of adsorbed species. *J. Phys. Chem. C.* **115**, 11540–11549 (2011).
32. Jahandar Lashaki, M., Khiavi, S. & Sayari, A. Stability of amine-functionalized CO_2 adsorbents: a multifaceted puzzle. *Chem. Soc. Rev.* **48**, 3320–3405 (2019).
33. Sayari, A., Heydari-Gorji, A. & Yang, Y. CO_2-induced degradation of amine-containing adsorbents: Reaction products and pathways. *J. Am. Chem. Soc.* **134**, 13834–13842 (2012).
34. Almassad, H. A., Abaza, R. I., Siwwan, L., Al-Maythalony, B. & Cordova, K. E. Environmentally adaptive MOF-based device enables continuous self-optimizing atmospheric water harvesting. *Nat. Commun.* **13**, 4873 (2022).
35. Shu, Q., Haug, M., Tedesco, M., Kuntke, P. & Hamelers, H. V. M. Direct air capture using electrochemically regenerated anion exchange resins. *Environ. Sci. Technol.* **56**, 11559–11566 (2022).
36. Buijs, W. & de Flart, S. Direct air capture of CO_2 with an amine resin: A molecular modeling study of the CO_2 capturing process. *Ind. Eng. Chem. Res.* **56**, 12297–12304 (2017).
37. Wurzbacher, J. A., Gebald, C., Piatkowski, N. & Steinfeld, A. Concurrent separation of CO_2 and H_2O from air by a temperature-vacuum swing adsorption/desorption cycle. *Environ. Sci. Technol.* **46**, 9191–9198 (2012).
38. Thomson, G. W. The Antoine equation for vapor-pressure data. *Chem. Rev.* **38**, 1–39 (1946).

Acknowledgements
This work is sponsored by the Australia Research Council DP190101336 (G.K.L.).

Author contributions
P.W., G.K.L., and Y.W. conceived the project. Y.W. performed the experiments. H.D., P.W., and G.K.L. supervised the work. Y.W., L.Q., and G.K.L. wrote the manuscript. All the authors contributed to discussions of the results and revisions of the manuscript.

Competing interests
Y.W., H.D., P.W., G.K.L., and the University of Melbourne submitted a patent application (No. PCT/AU2023/050429, filed on 22 May 2023) pertaining to the vapor promoted desorption process. L.Q. declares no competing interests.

Additional information
Supplementary information The online version contains supplementary material available at https://doi.org/10.1038/s41467-024-53961-4.

Correspondence and requests for materials should be addressed to Hui Ding, Paul Webley or Gang Kevin Li.

Peer review information *Nature Communications* thanks the anonymous reviewers for their contribution to the peer review of this work. A peer review file is available.